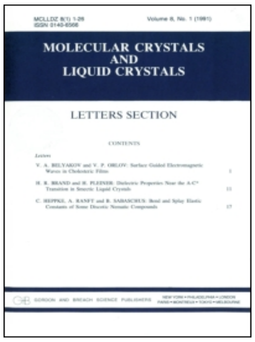

Molecular Crystals and Liquid Crystals

ISSN: 1542-1406 (Print) 1563-5287 (Online) Journal homepage: http://www.tandfonline.com/loi/gmcl20

# A bright yellow emissive dye configured by attaching triarylamine to naphthalimide with −NHN= bridge

Xiaochuan Li, Dandan Shan, Wooram Oh & Young-A Son

**To cite this article:** Xiaochuan Li, Dandan Shan, Wooram Oh & Young-A Son (2016) A bright yellow emissive dye configured by attaching triarylamine to naphthalimide with #NHN# bridge, Molecular Crystals and Liquid Crystals, 635:1, 172-180, DOI: 10.1080/15421406.2016.1200928

**To link to this article:** http://dx.doi.org/10.1080/15421406.2016.1200928

MOLECULAR CRYSTALS AND LIQUID CRYSTALS
2016, VOL. 635, 172–180
http://dx.doi.org/10.1080/15421406.2016.1200928

# A bright yellow emissive dye configured by attaching triarylamine to naphthalimide with –NHN= bridge

Xiaochuan Li[a], Dandan Shan[a], Wooram Oh[b], and Young-A Son[b]

[a]Collaborative Innovation Center of Henan Province for Green Manufacturing of Fine Chemicals, Key Laboratory of Green Chemical Media and Reactions, Ministry of Education, School of Chemistry and Chemical Engineering, Henan Normal University, Xinxiang, Henan, P. R. China; [b]BK21, Department of Advanced Organic Materials Engineering, Chungnam National University, South Korea

**ABSTRACT**

In this contribution, a dye (**TPN**) with 1,8-naphthalimide and triphenylamine incorporated together was linked by –*NHN*= bridge. It was fully characterized by NMR and HRMS spectroscopic techniques. Highly emissive character was observed in weak and medium polar solvent. The emission maximum varied from 494 (green) to 564 nm (orange). In polycarbonate film, **TPN** is also highly emissive with 550 nm emission peak. While in solid, the emission peak was shifted to red region due to the tightly molecular packing. The propeller like configuration of triphenylamine avoids regular packing and leads to the emission character in solid. Calculation of frontier molecular orbitals uncovers the underlying mechanism of solvatochromism.

**KEYWORDS**

1,8-naphthalimide; triphenylamine; highly emissive; molecular orbitals; solvatochromism

## Introduction

Small organic emissive molecules were configured and put into application by the chemists, physicists and biochemists in materials science and structural biotechnology. The potential of such molecules is significantly advanced by several typical families of highly emissive dyes that have been systematically engineered, such as coumarins, naphthalimide, bisindolylmalimide, cyanes, porphyrins, xanthenes, sauaraines, perylenediimides, and fluorine-boron complexes [1–13]. Due to the excellent photophyscial properties of the highly emissive dyes, widespread applications were developed in the field of organic electronics, OLEDs, nano-vehicles, photolectric transducer, bioimaging, and logical compiler [14–20].

1,8-naphthalimide (benz[*de*]isoquinolin-1,3diones) is one of the typical emissive dye mentioned above, which can be conveniently obtained from 1.8-naphthalic anhydrides by reaction with various alkylamine and have gone into mass production. Additionally, the framework of naphthalimide can be structurally modified at the 3- or 4-position, which allows the introduction of desired functional groups and exert major effect on the electronic properties with a consequent influence on the chemical, photochemical spectroscopic properties [21–23]. It also indicated that the optical and photophysical properties of 1,8-naphthalimide are very sensitive to substitution in aromatic ring. Generally, the emission of 1,8-naphthalimide

**CONTACT** Young-A Son yason@cnu.ac.kr Department of Advanced Organic Materials Engineering, Chungnam National University, 220 Gung-dong, Daejeon, 305-764, South Korea; Xiaochuan Li lixiaochuan@htu.cn School of Chemistry and Chemical Engineering, Henan Normal University, East Jianshe Rd. 46, Xinxiang, Henan, 453007, China.

Color versions of one or more of the figures in the article can be found online at www.tandfonline.com/gmcl.

derivatives is often in the green part of the electromagnetic spectrum and can be shifted toward red by altering the nature of the ring substituent or that of the imide. This yields particularly attractive emissive molecules since they can partially overcome auto-fluorescence and light scattering from biological environments. These tunable photophyscial properties make them excellent dye to probe the microenvironment as well as intensive investigation in the field of supramolecular chemistry.

In this contribution, triphenylamine, a propeller like electron donor unit, was attached to 1,8-naphthalimide with a −NHN= bridge. Our intention was to impose strong electronic effect on the core structure of naphthalimide and understood the corresponding properties through detailed study and structural analysis. Achieving the highly emissive molecules with shifted wavelength is of significant in the development of materials science and biotechnology.

## Experimental

### General procedures and materials

The solvents used in the reaction were carefully dried according to the standard procedure and stored over 4 Å molecular sieve. All the reagent-grade chemicals were purchased from Sigma-Aldrich CO. LLC. (South Korea) and used without further purification. Melting points were determined on a Mel-Temp® IA9200 digital melting point apparatus in a glass capillary and were uncorrected. All synthesized compounds were routinely characterized by TLC and $^1$H NMR. TLC was performed on aluminum-backed silica gel plates (Merck DC. Alufolien Kieselgel 60 F254).

### $^1$H and $^{13}$C NMR spectroscopy

$^1$H and $^{13}$C nuclear magnetic resonance (NMR) spectra were recorded on a Brucker AM-400 spectrometer operating at frequencies of 400 MHz for proton 100 MHz for carbon in $CDCl_3$. Proton chemical shifts ($\delta$) are relative to tetramethylsilane (TMS, $\delta = 0$) as internal standard and expressed in parts per million. Spin multiplicities are given as *s* (singlet), *d* (doublet), *t* (triplet), and *m* (multiplet) as well as *b* (broad). Coupling constants (*J*) are given in Hertz.

### High resolution mass spectra (HRMS)

The mass spectra measured on a LC-MS (Waters UPLC-TQD) mass spectrometer. High resolution mass spectra (HRMS) were measured on a Brucker micrOTOF II Focus instrument.

### UV-Vis and emission spectra

The absorption spectra were measured with a PERSEE TU-1900 and an Agilent 8453 spectrophotometer. Emission spectra were measured with Shimadzu RF-5301PC fluorescence spectrophotometer. The solvents used in photochemical measurement were spectroscopic grade and were purified by distillation. The stock solution of compounds ($2 \times 10^{-3}$ M) was prepared in THF, and a fixed amount of these concentrated solutions were added to each experimental solution. All the experiments were done repeatedly, and reproducible results were obtained. Prior to the spectroscopic measurements, solutions were deoxygenated by bubbling nitrogen through them.

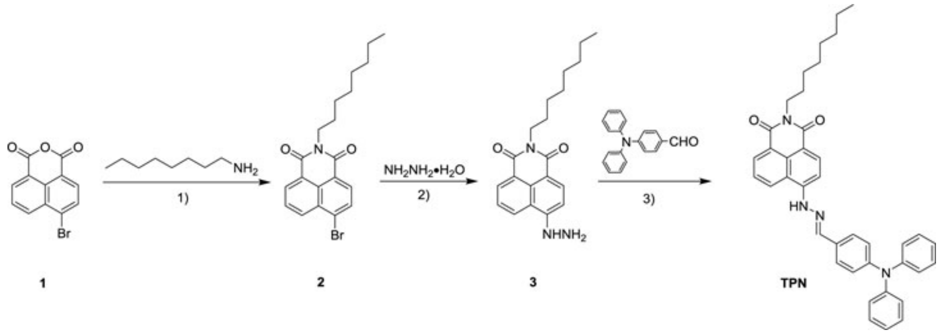

**Scheme 1.** Synthesis of 2-heptyl-6-(2-(4-(diphenylamino)benzylidene)hydrazinyl)-benzo[*de*]isoquinoline-1,3-dione (**TPN**). 1) *n*-octanamine, ethanol, reflux 4 h; 2) $NH_2NH_2 \cdot H_2O$, 2-methoxyethanol, reflux; 3) 4-formyltriphenylamine, toluene/isopropanol, rt.

### *Theoretical calculations*

For the theoretical study of the excited state photo-physics of the dye, the *DMol*$^3$ program, which is available as part of *Material Studio* (Accelrys Inc., San Diego, California, United States), was used. Both the ground state geometries and the frontier molecular orbital of the dye were calculated using the density function theory (DFT) with the B3LYP hybrid functional and the double numerical plus *d*-functions (DND) atomic orbital basis set.

## Synthesis

Synethetic routes of the target dye, 2-heptyl-6-(2-(4-(diphenylamino)benzylidene) hydrazinyl)-benzo[de]isoquinoline-1,3-dione (**TPN**), are outlined in Scheme 1. 4-Bromo-1,8-naphthalic anhydride (**1**) is commercially available and purchased from Aldrich and used as received. **2** (*N*-heptyl-4-bromo-1,8-naphthalimide) can be conveniently imidization with *n*-octanamine in ethanol, according to our previously report only with the different *N*-alkyl substituent [24, 25]. The active bromine atom of compound **2** was substituted by nitrogen atom of hydrazine hydrate and yielded **3** [25]. Finally, **3** was condensed with 4-formyltriphenylamine and yielded **TPN**.

### *2-heptyl-6-(2-(4-(diphenylamino)benzylidene)hydrazinyl)-benzo[de]isoquinoline-1,3-dione (TPN)*

*N*-Heptyl-6-hydrazinyl-1,8-naphthalimide (559 mg, 1.65 mmol) and 4-formyltriphenylamine (450 mg, 1.65 mmol) were mixed with toluene (20 mL) and isopropanol (8 mL). Next, the mixture was stirred at room temperature for 2 h. After the starting materials were full reacted, as confirmed by TLC, the mixed solvent was evaporated in a vacuum. The residue was purified by silica gel (200–300 mesh) column chromatography (eluent: dichloromethane), which produced pure samples of 835 mg (red powder, 85%).

Mp: 235–238°C; $^1$H NMR(400 MHz, $CDCl_3$): $\delta$ (ppm): 8.90 (1H, *b*), 8.55 (1H, *d*, $J = 8.0$ Hz), 8.50 (1H, *d*, $J = 8.0$ Hz), 8.21 (1H, *d*, $J = 8.0$ Hz), 8.03 (1H, *d*, $J = 8.0$ Hz), 7.68 (1H, *d*, $J = 8.0$ Hz), 7.62 (2H, *t*, $J = 8.0$ Hz), 7.36–7.29 (5H, *m*), 7.18–7.09 (6H, *m*), 7.05 (2H, *d*, $J = 8.0$ Hz), 4.14 (2H, *t*, $J = 8.0$ Hz), 1.71 (2H, *q*, $J = 8.0$ Hz), 1.42–1.38 (2H, *m*), 1.36–1.28 (9H, *m*), 0.86 (3H, *t*, $J = 8.0$ Hz). $^{13}$C NMR (100 MHz, $CDCl_3$): 164.6, 164.2, 147.0, 145.5, 134.1, 134.0, 131.5, 131.2, 131.1, 129.9, 129.7, 129.6, 128.5, 126.5, 126.0, 125.9, 125.4, 125.3, 125.2,

**Table 1.** Optical data of the **TPN** in various solvents.

| | UV-Vis | | Fluorescence | | |
|---|---|---|---|---|---|
| Solvent | $\lambda_{abs}$ (nm) | log $\varepsilon_{max}$ | $\lambda_{em}$ (nm) | $\Phi_F$ | Stokes shift (nm) |
| Hexane | 343 | 4.46 | | | |
| | 440 | 4.43 | 494 | 0.53 | 54 |
| Cyclohexane | 356 | 4.69 | | | |
| | 443 | 4.78 | 498 | 0.54 | 55 |
| Toluene | 345 | 4.64 | | | |
| | 434 | 4.28 | 530 | 0.82 | 96 |
| Dioxane | 357 | 4.60 | | | |
| | 460 | 4.73 | 540 | 0.90 | 80 |
| THF | 343 | 4.70 | | | |
| | 455 | 4.87 | 554 | 0.80 | 99 |
| Chloroform | 363 | 4.60 | | | |
| | 468 | 4.94 | 564 | 0.76 | 96 |
| *n*-BuOH | 360 | 4.83 | | | |
| | 485 | 5.00 | —[a] | —[b] | |
| Methanol | 358 | 4.66 | | | |
| | 479 | 4.81 | —[a] | —[b] | |
| DMSO | 362 | 4.55 | | | |
| | 482 | 4.74 | —[a] | —[b] | |
| Polycarbonate film | 350 | 4.65 | | | |
| | 456 | 4.80 | 550 | 0.51 | 94 |

[a,b] The data was not shown due to the weak emission.

124.2, 124.1, 122.1, 122.0, 119.4, 108.1, 40.5, 32.0, 29.5, 29.4, 28.3, 27.3, 22.7, 14.2. HRMS (ESI): $[M+Na]^+$ $C_{39}H_{38}N_4O_2Na$ requires 594.2995; found $[M+Na]^+$ 594.2990.

## Result and discussion

The stability and solubility of **TPN** were investigated in common organic solvents such as hexane, cyclohexane, toluene, dioxane, THF, chloroform, methanol, DMF, and DMSO. **TPN** exhibited good solubility and photostability in solvents. Even after 30 days of exposure to the room light, no color fading was observed. However, its spectroscopic properties were sensitive to the external environment. Significant solvatochromism was induced by the solvent polarity. The basic absorption/emission peaks, absorption coefficients, quantum yields, and Stokes shifts are presented in Table 1. The absorption spectra of **TPN** in various solvents were recorded in Figure 1. The longest absorption maximum varied from 440 to 468 nm with the solvent polarity varied. In nonpolar solvents (hexane and cyclohexane), the longest absorption maximum were located at ~440 nm. In comparison, the absorption position was shifted 15–28 nm toward the longer wavelength in medium polarity solvents (toluene, dioxane, THF, and chloroform). However, the molar extinction coefficients of **TPN** in different solvents are irregular. In toluene and hexane, the absorption in visible region is weaker than that in other solvents. Stronger absorption was observed in cyclohexane, dioxane, chloroform, and THF. The absorption of **TPN** in more polar solvents was also investigated (such as *n*-BuOH, methanol, and DMSO) and similar absorption profiles were found, except for the difference in absorptivities. Also, the absorption position was significantly shifted to ~480 nm.

The emission of **TPN** is significantly environment dependent. In high polar solvent (such as *n*-BuOH, MeOH, and DMSO), the emission of **TPN** was almost quenched totally. However, it is highly emissive in weak or medium polarity solvent, such as hexane, cyclohexane, toluene, dioxane, THF, and chloroform. Detailed emission properties are listed in Table 1. Figure 2 shows the emission spectra of **TPN** in different solvents, with which highly emission

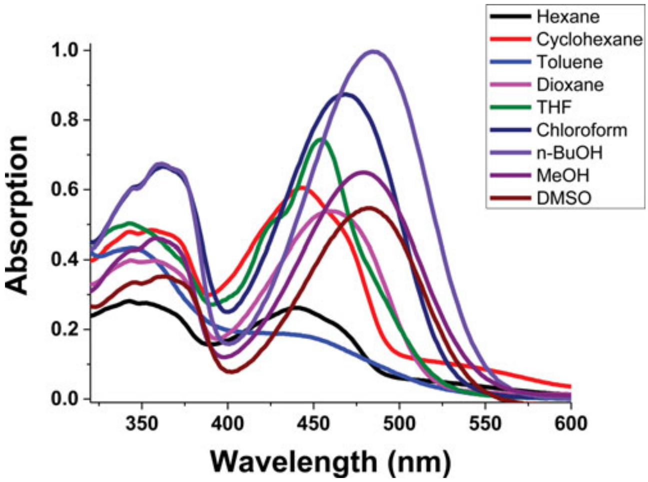

**Figure 1.** Absorption spectra of **TPN** in various solvents ($1.0 \times 10^{-5}$ M).

was induced. **TPN** exhibited an obvious positive solvatochromism from nonpolar hexane to medium polar chloroform. According to Figure 2, the emission maxima of **TPN** were varied from 494 to 564 nm. In hexane and cyclohexane, the emission profiles are almost identical to each other, which are composed of high- and low-energy emission bands with the former stronger that the latter. From hexane to cyclohexane, only 4 nm red-shifted emissions were induced due to a slight change in solvent polarity. Further red-shifting was observed with the increase of polarity of solvents. Interestingly, the emission maximum was shifted towards longer wavelength in ~10 nm increment (530 nm→540 nm→554 nm→564 nm), inducing by the solvents and following the order toluene<dioxane<THF<chloroform. It is known to all that the solvatochromism depends on the molecular structure, the nature of the chromophores, as well as the solvents [26]. The positive solvatochromism with increasing solvent polarity indicates that the dipole moment of the molecule in the excited state ($\mu_e$) is expected to be higher than that of the ground state ($\mu_g$). The quantum yields of **TPN** in different solvents varied in the range of 0.53–0.90. In contrast, **TPN** is highly emissive in dioxane than

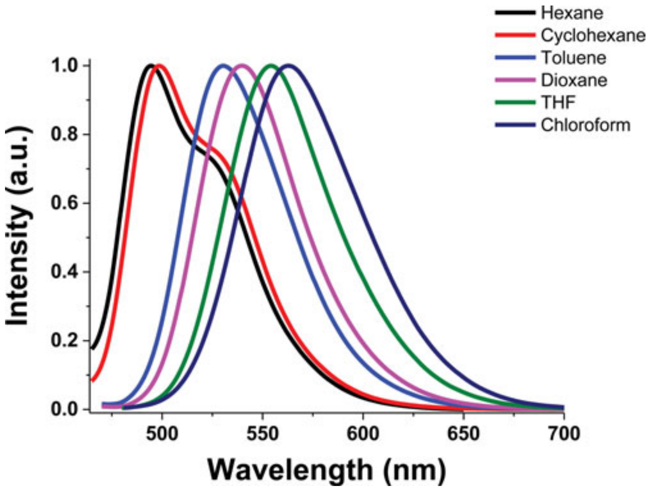

**Figure 2.** Emission spectra of **TPN** in various solvents ($1.0 \times 10^{-5}$ M).

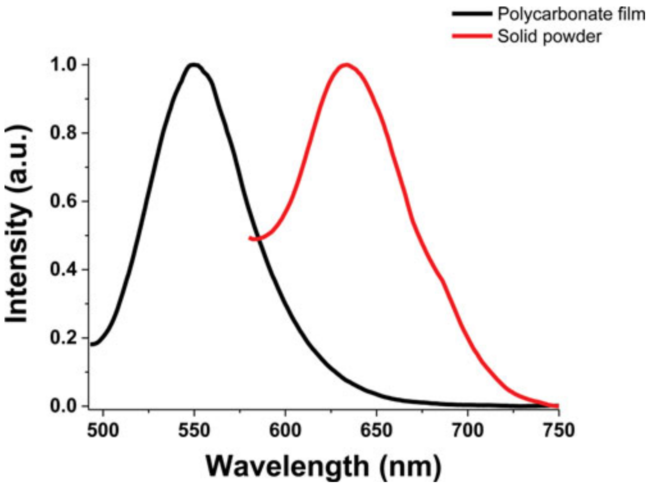

**Figure 3.** Emission spectra of **TPN** in film with 5 -wt.% in polycarbonate and in solid powder.

that in other solvents. In medium polar environment, the emission efficiency is stronger. It verifies that the medium polar environment could stabilize the excited state of **TPN** better than that of the ground state, and thus, a lower energy gap between these electronic states and longer wavelength emission. With the polarity of environment increasing or decreasing, the emission will be totally or partially quenched, for example, in methanol (proton polar solvent) and DMSO (non-proton polar solvent). The variation trend of emission efficiency also indicates that the excited **TPN** can be stabilized better in medium polar environment, which leads to the higher quantum yields. In nonpolar solvents, this stabilization gets weaker. While in high polar solvents, the stronger polar environment intensifies the interaction between the solute and the solvent molecules and the nonradiative transition from the excited states to the ground states is also intensified, and leads to emission quench (very low quantum yield).

**TPN** is also emissive in film blended with polycarbonate and in the solid powder state and the emission spectra are shown in Figure 3. The emission **TPN** in film blended in polycarbonate (5 -wt.%) exhibited similar profile and maximum peak to that in THF. Compared to the emission in nonpolar solvent (hexane/cyclohexane), the emission maximum in polycarbonate film was bathochromic shift about 50nm. Both the polar environment and the irregular tight packing in polycarbonate matrix contribute to the emission bathochromic shift [27]. In the solid powder state, the emission maximum was further red-shift to 633 nm, indicating tighter packing than that of film. Additionally, the emission in solid powder was significantly broadened, with the full with at half maximum (FWHM) reaching to 83 nm (broader than that of polycarbonate film 65 nm). The highly emissive character in polycarbonate film is attractive for **TPN** because benzenes are potential dopant emitters in host materials. The emission color changes in solution/film/solid powder were characterized by CIE coordinates (Figure 4). In solution, the emission color varied from green to orange induced by polarity of solvents, which is in agreement with the CIE coordinates distribution. A notable CIE coordinate change of **TPN** was observed in solid powder and moved to red region due to the tight molecular packing.

To better comprehend the geometrical, electronic, and optical properties of **TPN**, we undertook a comprehensive computational investigation using Material Studio. To reduce the run times in the first instance, the ground-state energy-minimized structures were calculated

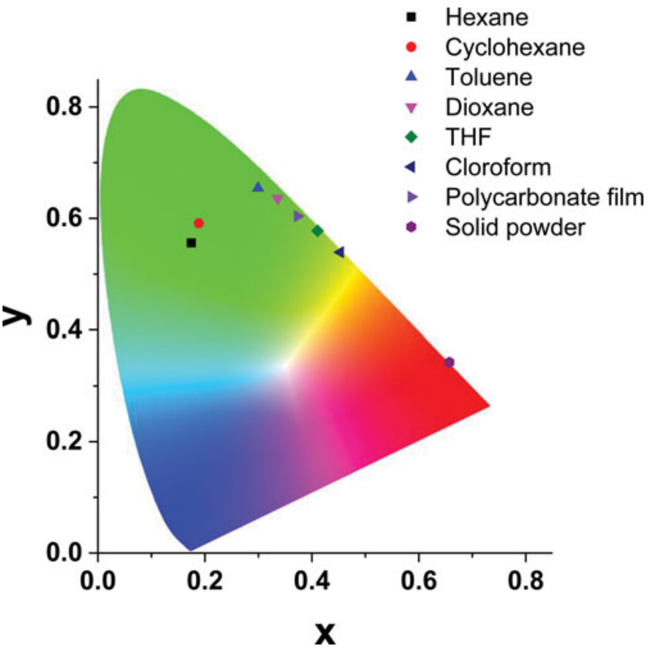

**Figure 4.** CIE 1931 chromaticity diagram of the emissions of **TPN** in solution/polycarbonate film/solid powder.

using DFT and LDA/DN basis set [28, 29]. Further refinement and optimization on structures were undertaken using DND/B3LYP basis set.

The size and signs of frontier molecules orbitals of **TPN** are illustrated in Figure 5. Only the highest occupied molecular orbitals (HOMO) and lowest unoccupied molecular orbitals (LUMO) were calculated because the strong absorption bands in the visible region are generally dominated by HOMO to LUMO excitation [4, 30, 31]. In Figure 5, distinctive contributions of each atomic orbital are discernible in the HOMO and LUMO diagrams. In HOMO, the electron density is well distributed over the triphenylamine and the bridging unit (–*NHN*=),

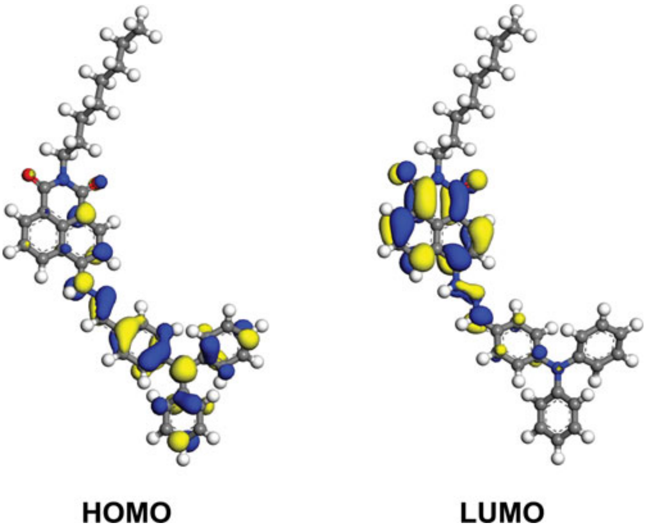

**Figure 5.** HOMO and LUMO diagrams of **TPN** obtained from *DMol*$^3$ calculations.

reflecting the electron-donating nature of triphenylamine unit. Only a small amount of electron density spread to naphthalimide unit. The LUMO distribution is distinctly different form that of HOMO. The naphthalimide (electron-acceptor) and the bridging unit (*−NHN=*) contribute completely to the LUMO. A bridge was established by the electron rich unit (*−NHN=*), which contribute always to the HOMO/LUMO distribution. Due to the larger difference in HOMO/LUMO distribution, the charge transfer (CT) process is characteristically sensitive to solvent polarities. The typical CT character is the identified solvatochromism – change in transition frequency with change in solvent dielectric constant. In nonpolar conditions, the excitation of **TPN** is less interacted. While in medium polar conditions, the excited state of **TPN** will be interacted and enhance the non-radiative transition pathway. Therefore, a gradually lowered emission was observed in toluene/dioxane/THF/chloroform. If the strong polar condition was applied to **TPN**, the excited of **TPN** will be disturbed significantly by vibrated dipole moment and most of the energy was lost due to the nonradiation, resulting to very weak emission. In polycarbonate film, the molecule packing is tighter than that in solution, together with the polar polycarbonate matrix, shifted the emission band to orange. At the same time, the propeller-like of triphenylamine resists the regular packing of **TPN**, and thus avoiding emission quench, which is in agreement with the highly emissive character in polycarbonate film. In solid powder state, it is the more tightly irregular packing disturbing the excited state. Intermolecular interaction will lead to the configuration transformation and lowered the emission energy, leading to significant emission shift to the red region.

## Conclusions

In summary, a new *2*-heptyl-6-(2-(4-(diphenylamino)benzylidene)hydrazinyl)-benzo[de]-isoquinoline-1,3-dione (**TPN**) was synthesized and fully characterized. A long alkyl chain was introduced to naphthalimide unit, enhancing the solubility in organic medium. Triphenylamine, was attached with *−NHN=* as the bridging unit, acting as an electron-donator. The absorption and emission of **TPN** in various solvents were investigated. **TPN** is highly emissive in nonpolar and medium nonpolar solvents. Particularly, it is most emissive for **TPN** in dioxane with the emission maximum at 540 nm. In polycarbonate film, **TPN** is also highly emissive with similar emission peak (550 nm) to that in dioxane. Due to the tightly molecular packing in solid, the emission maximum was further shifted to the red region (633 nm). The emission color of **TPN** in solution/film/solid powder was characterized by CIE coordinates in detail. Computational results of frontier orbitals suggest that there is large difference in HOMO/LUMO distributions. It indicates that the excitation and excited state of **TPN** is easy to be interfered by the polar conditions induced by the solvents or polymer matrix. Our efforts towards the application of **TPN** in device fabrication and biological purpose are currently underway.

## Acknowledgments

This work was supported by the National Natural Science Foundation of China (21272060), PCSIRT (grant no. IRT1061), and the Program for Innovative Research Team in University of Henan Province (15IRTSTHN003). This study was supported by the Basic Science Research Program through the National Research Foundation of Korea (NRF) funded by the Ministry of Science, ICT and Future Planning (Grant No. 2015021972).

## References

[1] Sethna, S. M., & Shah, N. M. (1945). *Chem. Rev.*, *36*, 1.
[2] Banerjee, S., Veale, E. B., Phelan, C. M., Murphy, S. A., Tocci, G. M., Gillespie, L. J., Frimannsson, D. O., Kelly, J. M., & Gunnlaugsson, T. (2013). *Chem. Soc. Rev.*, *42*, 1601.
[3] Oelgemoller, M., & Kramer, W. H. (2010). *J. Photoch. Photobio. C.*, *11*, 210.
[4] Li, X., Xu, Y., Wang, B., & Son, Y. -A. (2012). *Tetrahedron Lett.*, *53*, 1098.
[5] Li, X., Zhu, K., Li, Y., Kim, H., & Son, Y. -A. (2013). *Mol. Cryst. Liq. Cryst.*, *584*, 18.
[6] Li, X., Shi, R., Jin, Y., Lou, Y., Ge, Q., Li, M., Kim, H., & Son, Y. -A. (2014). *J. Nanosci. Nanotechnol.*, *14*, 8033.
[7] Mishra, A., Behera, R. K., Behera, P. K., Mishra, B. K., & Behera, G. B. (2000). *Chem. Rev.*, *100*, 1973.
[8] Wasielewski, M. R. (1992). *Chem. Rev.*, *92*, 435.
[9] Beija, M., Afonso, C. A. M., & Martinho, J. M. G. (2009). *Chem. Soc. Rev.*, *38*, 2410.
[10] Beverina, L., & Salice, P. (2010). *Eur. J. Org. Chem.*, *7*, 1207.
[11] Weil, T., Vosch, T., Hofkenes, J., Peneva, K., & Müllen, K. (2010). *Angew. Chem. Int. Ed.*, *49*, 9068.
[12] Li, X., & Son, Y. -A. (2014). *Dyes Pigm.*, *107*, 182.
[13] Li, X., Ji, G., & Son, Y. -A. (2016). *Dyes Pigm.*, *124*, 232.
[14] Goze, C., Ulrich, G., & Ziessel, R. (2007). *J. Org. Chem.*, *72*, 313.
[15] Li, G., Zhao, Y., Li, J., Cao, J., Zhu, J., Sun, X. W., & Zhang, Q. (2015). *J. Org. Chem.*, *80*, 196.
[16] Osken, L., Gundogan, A. S., Tekin, E., Eroglu, M. S., & Ozturk, T. (2013). *Macromolecules.*, *46*, 9202.
[17] Zhang, Y., Swaminathan, S., Tang, S., Garcia-Amorós, J., Boulina, M., Captain, B., Baker, J. D., & Raymo, F. M. (2015). *J. Am. Chem. Soc.*, *137*, 4709.
[18] Maniam, S., Holmes, A. B., Leeke, G. A., Bilic, A., & Collis, G. E. (2015). *Org. Lett.*, (in press).
[19] Chen, W., Rosser, E. W., Zhang, D., Shi, W., Li, Y., Dong, W. -J., Ma, H., Hu, D., & Xian, M. (2015). *Org. Lett.*, *17*, 2776.
[20] Liu, G. -F., & Feng, C. -L. (2015). *Langmuir.*, *31*, 7122.
[21] Li, X., & Son, Y. -A. (2015). *J. Nanosci. Nanotechnol.*, *15*, 5370.
[22] Li, X., & Son, Y. -A. (2014). *Mol. Cryst. Liq. Cryst.*, *604*, 184.
[23] Li, X., Zhang, Y. Zhao, N., & Son, Y. -A. (2014). *Mol. Cryst. Liq. Cryst.*, *600*, 163.
[24] Zhao, Y., & Li, X. (2015). *Sensors & Actuators, B: Chemical.*, *209*, 258.
[25] Cao, J., & Wang, X. -M. (2013). *Tetrahedron.*, *69*, 10267.
[26] Hartmann, H., Eckert, K., & Schröder, A. (2000). *Angew. Chem. Int. Ed.*, *39*, 556.
[27] Shundo, A., Okada, Y., Lto, F., & Tanaka, K. (2012). *Macromolecules.*, *45*, 329.
[28] Delley, B. (1990). *J. Chem. Phys.*, *92*, 508.
[29] Delley, B. (2000). *J. Chem. Phys.*, *113*, 7756.
[30] Inari, T., Yamano, M., Hirano, A., Sugawa, K., & Otsuki, J. (2014). *J. Phys. Chem.*, *118*, 5178.
[31] Stock, R. I., Nandi, L. G., Nicoleti, C. R., Schramm, A. D. S., Meller, S. L., Heying, R. S., Coimbra, D. F., Andriani, K. F., Caramori, G. F., Bortoluzzi, A. J., & Machado, V. G. (2015). *J. Org. Chem.*, *80*, 7971.